ELSEVIER

Biochemical Pharmacology 64 (2002) 595–607

Biochemical Pharmacology

Inhibition of the activity of T lymphocyte Kv1.3 channels by extracellular zinc

Andrzej Teisseyre*, Jerzy W. Mozrzymas

Department of Biophysics, Wrocław Medical University, ul. Chałubińskiego 10, 50-368 Wrocław, Poland

Received 27 March 2002; accepted 30 April 2002

Abstract

The inhibitory effect of zinc on voltage-gated Kv1.3 channels in human T lymphocytes was investigated using the ''whole-cell'' patch-clamp technique. Application of 10 and 20 μM Zn caused a concentration-dependent shift of activation midpoint of the whole-cell currents from -19.65 ± 1.03 mV (mean ± SE) under control conditions to 9.84 ± 0.66 mV upon application of 20 μM Zn. This effect was saturated at zinc concentrations higher than 20 μM. The activation rate was considerably slower, whereas the deactivation rate was not significantly affected by Zn. Inactivation midpoint was shifted from -53.06 ± 0.44 mV under control conditions to -36.05 ± 0.48 mV in the presence of 100 μM Zn. Inactivation rate was not significantly affected upon Zn treatment. Whole-cell potassium currents were reduced to about 70% of their control values with no clear concentration dependence in the zinc concentration range from 10 to 100 μM. When raising the zinc concentration to levels above 100 μM, a concentration-dependent inhibition of the whole-cell currents appeared additionally to the changes in channel gating. The channels were half-blocked at the zinc concentration of 346 ± 40 μM and the Hill slope coefficient was 1.89 ± 0.21. The inhibitory effect of zinc was not complete at micromolar concentrations and was saturated at concentrations higher than 1 mM. This inhibitory effect was not accompanied by any further modification in the shift of the activation and inactivation midpoints nor by a slowing of the channel activation rate. The inhibitory effect of zinc was significantly diminished in the presence of 150 mM K^+ in the extracellular solution, whereas the zinc-induced shift of the activation threshold and slowing of the activation kinetics remained unchanged when raising extracellular potassium concentration. It is suggested that zinc acts on two independent binding sites on the channels. Binding to one site that is saturated at concentrations higher than 20 μM affects the channel gating. Binding to another site at concentrations higher than 100 μM inhibits the currents without affecting the channel gating.

Keywords: Zinc; Potassium channel; T lymphocyte; Patch-clamp

1. Introduction

Zinc is known as an important co-factor or structural component of more than 200 enzymes and several non-enzymatic proteins. It is also known as a potent endogenous modulator of many types of ion channels. Among them are: $GABA_A$ and NMDA receptors, voltage-gated sodium, potassium and calcium channels, inward rectifier and ATP-regulated potassium channels, ligand and voltage-gated ''maxi'' chloride channels (reviewed in [1]).

Studies on modulatory effects of zinc on the activity of voltage-gated potassium channels were first performed on the channels expressed in squid giant axons [2]. The results provided evidence that zinc application at millimolar concentrations (2–50 mM) considerably slowed channel opening and reduced whole-cell potassium currents without significantly affecting channel closing, suggesting specific interactions of zinc ions with channel gating charge that led to a stabilisation of the channel closed states [2]. This hypothesis was then confirmed in experiments performed by Spires and Begenisich (1992, 1994), who reported that zinc and other divalent cations bind to specific sites and directly influence gating kinetics; the

* Corresponding author. Tel.: +48-71-784-1414; fax: +48-71-784-0088.
E-mail address: ateiss@biofiz.am.wroc.pl (A. Teisseyre).

Abbreviations: TL, human T lymphocyte; 4-AP, 4 aminopyridine; gK, chord conductance; gK_{rel}, relative chord conductance; $gK_{contr60}$, chord conductance recorded on the same cell under control conditions at the membrane potential of +60 mV; gK_{norm}, normalised chord conductance; I_p, amplitude of the current; V, membrane potential; V_{rev}, reversal potential of the current; gK_{max}, maximal relative chord conductance; V_n, activation midpoint; k_n, steepness of the voltage dependence (activation); τ_n, activation time constant; $I_{p\ max,}$ peak current recorded at +40 mV from the holding potential of −120 mV; V_i, inactivation midpoint; k_i, steepness of the voltage dependence (inactivation).

0006-2952/02/$ – see front matter © 2002 Published by Elsevier Science Inc.
PII: S0006-2952(02)01227-3

binding effect occurs in competition with H^+ ions and amino groups are involved in the binding [3,4].

Application of zinc at micromolar concentrations was shown to affect the gating kinetics of *Shaker* potassium channels [4], transient voltage-gated potassium currents (I_A currents) recorded in acutely dissociated neurons from suprachiasmatic nucleus [5], granule cells from rat cerebellar slices [6] and snail neurons [7]. In all the cases zinc affected the channel gating producing a pronounced shift of steady-state activation and inactivation curves towards more positive potentials and slowing the activation kinetics without considerably affecting deactivation kinetics. Modulation of channel gating by micromolar zinc concentrations was also reported for voltage-gated cloned rat Kv1.1 and human Kv1.5 delayed rectifier channels and human inactivating Kv1.4 channels stably expressed in mouse fibroblasts [8]. Zinc application caused a shift of steady-state activation curves towards more positive potentials and a considerable reduction of the whole-cell current. Moreover, Zn application shifted the steady-state inactivation curve of Kv1.4 channels towards more positive potentials and considerably slowed the activation kinetics of Kv1.5 channels [8]. However, not all types of voltage-gated potassium channels are affected by zinc, for example, Kv1.2 channels are insensitive to zinc ions [1].

Voltage-gated Kv1.3 channels are the predominating potassium channels expressed in mouse, rat and human T lymphocytes (TL); these channels are also present in rat and mouse brain cells (reviewed in [9]). Kv1.3 channels play an important role in the cell function. Obtained data provide evidence that the activity of Kv1.3 channels is essential for setting the resting membrane potential in TL [9]. Kv1.3 channels are also required for the cell mitogenesis and volume regulation [9]. It is known that blockade of Kv1.3 channels also blocks both the cell mitogenesis and volume regulation [9]. Therefore, some non-peptide Kv1.3 channel blockers might have been used as immunosuppresive agents [9].

It is known that divalent and polyvalent cations inhibit whole-cell potassium currents and change gating kinetics of TL Kv1.3 channels [10–14]. The ions act at different concentrations with apparently different mechanisms [10–14]. Zinc was also mentioned as TL Kv1.3 channel inhibitor [10]. However, the mechanism of the inhibitory effect of zinc on Kv1.3 channels was not studied in a further detail.

Taking into account the importance of Kv1.3 channel activity for TL function it was of interest to investigate the mechanism of an inhibitory effect of zinc on Kv1.3 channels in human TL. Our results demonstrate that extracellular zinc inhibits, but not completely blocks the activity of TL Kv1.3 channels at micromolar concentrations. It is suggested that zinc acts on two independent binding sites on the channels. Binding to one site that is saturated at concentrations higher than 20 μM affects the channel gating. Binding to another site at concentrations higher than 100 μM produces an additional inhibitory effect on the currents without affecting the channel gating.

Results of this study have been published in the abstract form [15].

2. Materials and methods

2.1. Cell separation, solutions and pipettes

Human TL were separated from peripheral blood samples from eight healthy donors using a standard method described elsewhere [16]. After separation, cells were cultured for at least 24 hr in the standard RPMI-1640 Medium (SIGMA) supplemented with 5% v/v horse serum (SIGMA).

Upon experiment, cells were placed in the external solution containing (in mM: 150 NaCl, 4.5 KCl, 1 $CaCl_2$, 1 $MgCl_2$, 10 HEPES; pH = 7.35, 300 mOsm). A modified solution with increased concentrations of divalent cations (in mM: 140 NaCl, 4.5 KCl, 4 $CaCl_2$, 5 $MgCl_2$, 10 HEPES; pH = 7.35, 300 mOsm) was also used in several experiments. In another series of experiments, a solution containing 150 mM KCl, 1 mM $CaCl_2$, 1 mM $MgCl_2$, 10 mM HEPES; pH = 7.35, 300 mOsm, was used. The pipette solution contained 70 mM KF, 80 mM KCl, 1 mM $CaCl_2$, 1 mM $MgCl_2$, 10 mM HEPES, 10 mM EGTA; pH = 7.2, 280 mOsm. The free calcium concentration in the internal solution was calculated to be 100 nM. The chemicals were provided by the Polish Chemical Company (POCH), except HEPES, EGTA, 4-AP and clotrimazole that were purchased from SIGMA. Dishes with cells were placed under an inverted Olympus IMT-2 microscope. Zinc containing solutions ($ZnCl_2$) were applied using a fast perfusion system RSC 200 (Bio-Logic). Pipettes were pulled from the borosilicate glass (Hilgenberg) and fire-polished before the experiment. The pipette resistance was in the range of 3–5 MΩ.

2.2. Electrophysiological recordings

Whole-cell potassium currents in TL were recorded by applying the patch-clamp technique [17]. The currents were recorded using an EPC-7 Amplifier (List Electronics), low-pass filtered at 3 kHz, digitised using the LAB MASTER TL-1 (Axon Instruments) analog-to-digital converter with the sampling rate of 10 kHz and stored on the computer hard disk. A standard protocol of depolarising voltage stimuli contained seven pulses in the voltage range from −60 to +60 mV (20 mV increment) applied every 10 s, pulse duration 50 ms, holding potential −90 mV. In experiments performed with the presence zof 150 mM K^+ in the extracellular solution, the pulse duration was reduced to 40 ms. In order to check-out whether the 10 s interpulse interval is sufficient to avoid the use-dependent inactivation of Kv1.3 channels [9], we performed a series of experiments under control conditions, in which the currents

were recorded by applying the same depolarising protocols with 10 and 30 s interpulse intervals. Obtained data demonstrate that the currents recorded when applying a 10 s interpulse interval did not differ significantly from those obtained with 30 s interval. Results of experiments performed under control conditions provided evidence that stable whole-cell currents can be recorded under our experimental conditions up to ca. 20 min. Inactivation kinetics were studied by applying another protocol containing seven long-lasting (1 s) depolarising pulses applied every 30 s in the range from 0 to +60 mV (10 mV increment, holding potential −90 mV). The linear (ohmic) component of the current was subtracted online by applying the P/4 procedure. Steady-state inactivation was investigated by recording the currents at fully depolarising potential (+40 mV) after having applied various holding potentials in the range from −120 to 0 mV (10 mV increment) for 40 s. Reversal potential and deactivation kinetics were estimated by applying a tail current protocol: every 10 s the membrane was briefly (30 ms) depolarised to +40 mV from the holding potential of −90 mV to fully activate the currents and then repolarised to various potentials in the range from −50 to −90 mV (pulse duration 100 ms, 10 mV increment). In order to present more clearly the reversal of the currents, a modified protocol was applied every 10 s the cells were briefly (20 ms) depolarised to +40 mV (holding potential −90 mV) and then repolarised in the voltage range from −60 to −120 mV (pulse duration −80 ms, 10 mV increment).

The data are given as mean ± standard error.

All experiments were carried out at room temperature (22–24°).

2.3. Data analysis and curve fitting

When analysing the data of experiments with zinc application, only the results obtained on cells that displayed stable whole-cell currents in the absence of zinc—before zinc application and after wash-out—were taken into consideration. Records taken on some cells that displayed the ''run-down'' phenomenon or were lost after a couple of minutes of recording were excluded from the analysis. Since the number of active channels was varying significantly among the cells, steady-state activation of the channels was presented in terms of a relative chord conductance (gK_{rel}) defined by an equation $gK_{rel} = gK/gK_{contr60}$, where gK: chord conductance and $gK_{contr60}$: chord conductance recorded on the same cell under control conditions at the membrane potential of +60 mV. In order to demonstrate more clearly the shift in the activation threshold in the presence of Zn, the relative chord conductance was normalised to 1 at +60 mV and termed as normalised chord conductance (gK_{norm}). The chord conductance was calculated according to the definition $gK = I_p/(V - V_{rev})$, where I_p: amplitude of the current, V: membrane potential and V_{rev}: reversal potential of the current. The voltage dependence of steady-state activation was fitted by a Boltzmann function given by an equation $gK_{rel}(V) = gK_{max}/(1 + \exp(-((V - V_n)/k_n)))$, where gK_{max}: maximal relative chord conductance (in case of normalised chord conductance equal to 1), V_n: activation midpoint and k_n: steepness of the voltage dependence. The activation kinetics were fitted by applying the sigmoidal power function given by an equation $I(t) = I_p(1 - \exp(-t/\tau_n))^4$, where τ_n is activation time constant. Steady-state inactivation was presented in terms of the relative peak current defined as: $I_{p\,rel} = I_p/I_{p\,max}$, where $I_{p\,max}$ is the peak current recorded at +40 mV from the holding potential of −120 mV. The voltage dependence of steady-state inactivation was fitted by a Boltzmann function as in the case of steady-state activation with the inactivation midpoint (V_i) applied instead of V_n and steepness (k_i) applied instead of k_n.

3. Results

Fig. 1A shows an example of the whole-cell potassium currents recorded in TL under control conditions by applying a standard protocol of depolarising voltage stimuli described in Section 2. For clarity, only the first 30 ms of the current traces are presented on the graphs. The currents are evoked by membrane depolarisation from the holding potential of −90 mV to voltages more positive than −40 mV and fully activated at all potentials more positive than −20 mV. The currents reversed at potentials ca. −80 mV (see below). This value is close to the equilibrium potential for potassium ions under our experimental conditions calculated by applying the Nernst's equation (−87 mV). The currents are almost completely (>95%) blocked upon application of 5 mM 4-AP, which selectively blocks Kv1.3 channels in human TL (see Fig. 1B) [9,18]. This is in agreement with previous studies [9]. The blocking effect of 4-AP is reversible (data not shown). It is known that intermediate-conductance calcium-activated potassium channels termed IKCa1 are expressed abundantly in mitogen-activated, but not in quiescent TL [19]. IKCa1 channels are selectively blocked by clotrimazole at nanomolar concentrations [19]. Our results demonstrate that application of 500 nM clotrimazole does not reduce the currents significantly (see Fig. 1C). These results confirm that the currents recorded in our experiments are predominantly due to activation of Kv1.3 channels and argue against any significant contribution of IKCa1 currents. Moreover, it is worthy to note that our internal solution contains 10 mM EGTA (see Section 2) that keeps the intracellular free calcium concentration at the level of 100 nM [9]. According to the available data, any massive activation of calcium-dependent potassium channels is unlikely under such experimental conditions [9].

When recording the whole-cell currents in TL, chloride currents due to an activation of ''maxi'' voltage-gated

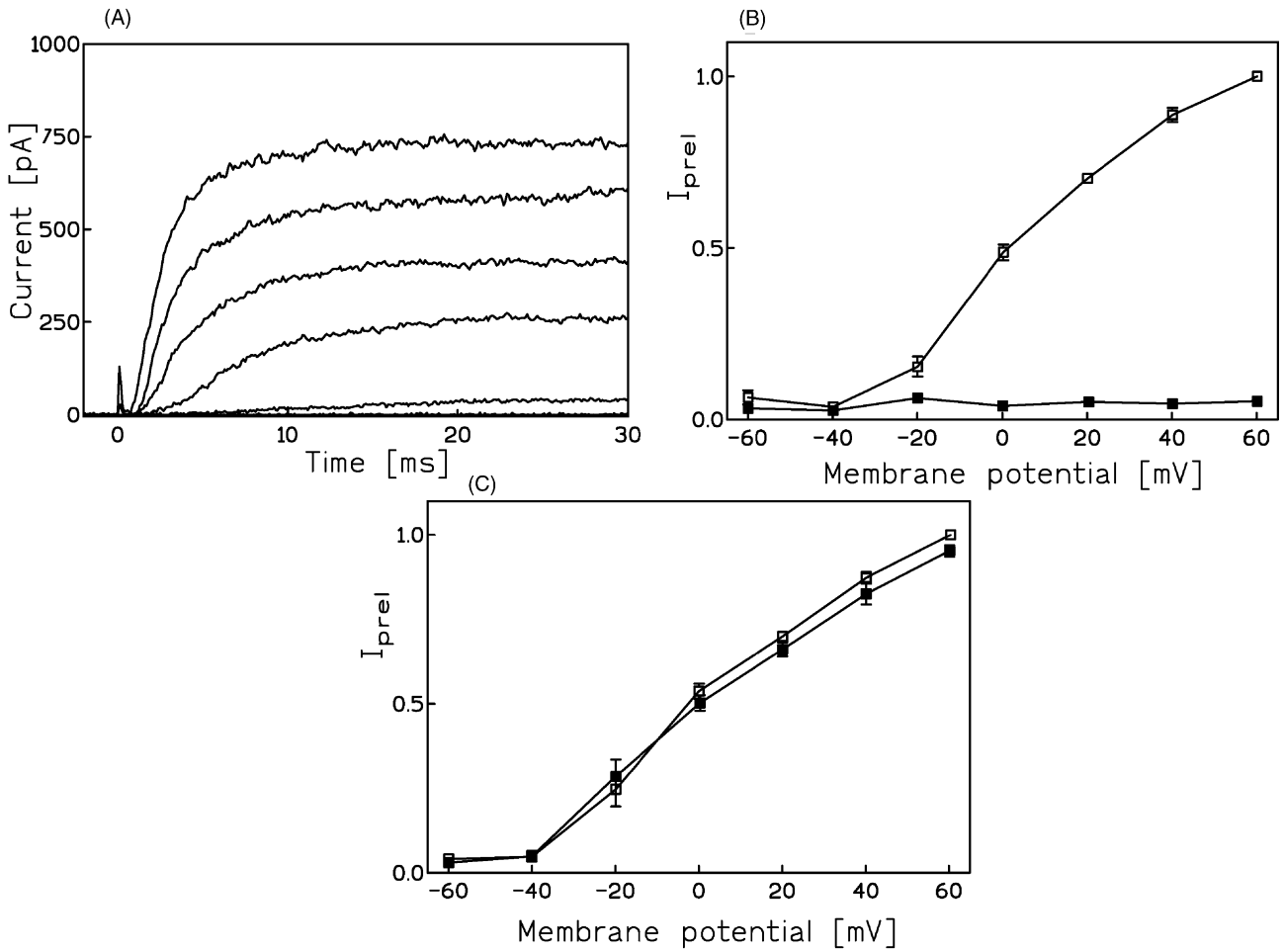

Fig. 1. (A) Whole-cell potassium currents in human TL recorded by applying a standard depolarising voltage protocol described in Section 2 under control conditions. (B) Relative peak current to voltage dependence; open squares: control conditions (N = 6), closed squares: application of 5 mM 4-AP (N = 6). (C) Relative peak current to voltage relationship; open squares: control conditions (N = 5), closed squares: application of 500 nM clotrimazole (N = 5). The data points in (B) and (C) was fitted by a point-to-point line.

chloride channels may appear additionally to the potassium currents [20]. However, the reversal potential for chloride ions under experimental conditions was estimated to be ca. −35 mV, that is far from −80 mV observed in our experiments. This argue against any significant contribution of the chloride current to the total whole-cell current (see also below).

Effects of application of 20 μM extracellular Zn on the channel gating is presented on Fig. 2. Fig. 2A shows a record taken under control conditions, whereas Fig. 2B depicts the effects of zinc treatment. It can be seen that the threshold of channel activation is markedly shifted towards more positive potentials; the currents were evoked only at the potentials more positive than 0 mV upon Zn application. Moreover, the activation kinetics of the currents were apparently slower upon Zn treatment compared to control conditions and the current amplitudes were reduced to about 70% of their control values. The effects of Zn was completely reversible (see Fig. 2C).

In order to demonstrate more clearly the effects of Zn on the channel currents and gating, various Zn concentrations were applied. Fig. 3A shows the effects of Zn applied at concentrations of 10, 20 and 100 μM on steady-state activation (measured as the relative chord conductance defined in Section 2) as a function of the membrane potential. A concentration-dependent shift of the activation midpoint (V_n) value towards more positive membrane potentials is clearly observed. Application of 10 μM Zn shifts the V_n from −19.65 ± 1.03 mV (N = 30) under control conditions to −2.15 ± 1.46 mV (N = 6). Raising the Zn concentration to 20 μM, and 100 μM shifted the V_n value to 8.45 ± 0.48 mV (N = 6) and 13.75 ± 2.59 mV (N = 30), respectively. The shift in the V_n value is better seen on Fig. 3B, where the normalised chord conductances (gK_{norm}) were plotted as a function of the membrane potential. Moreover, Zn application apparently reduced the whole-cell current amplitudes with no clear concentration dependence in that concentration range (see Fig. 3A). Upon application of 10, 20 and 100 μM Zn the peak value of the relative chord conductance was 0.67 ± 0.17 (N = 6), 0.76 ± 0.24 (N = 6) and 0.74 ± 0.03 (N = 30) of the control value, respectively. The steepness of the steady-state

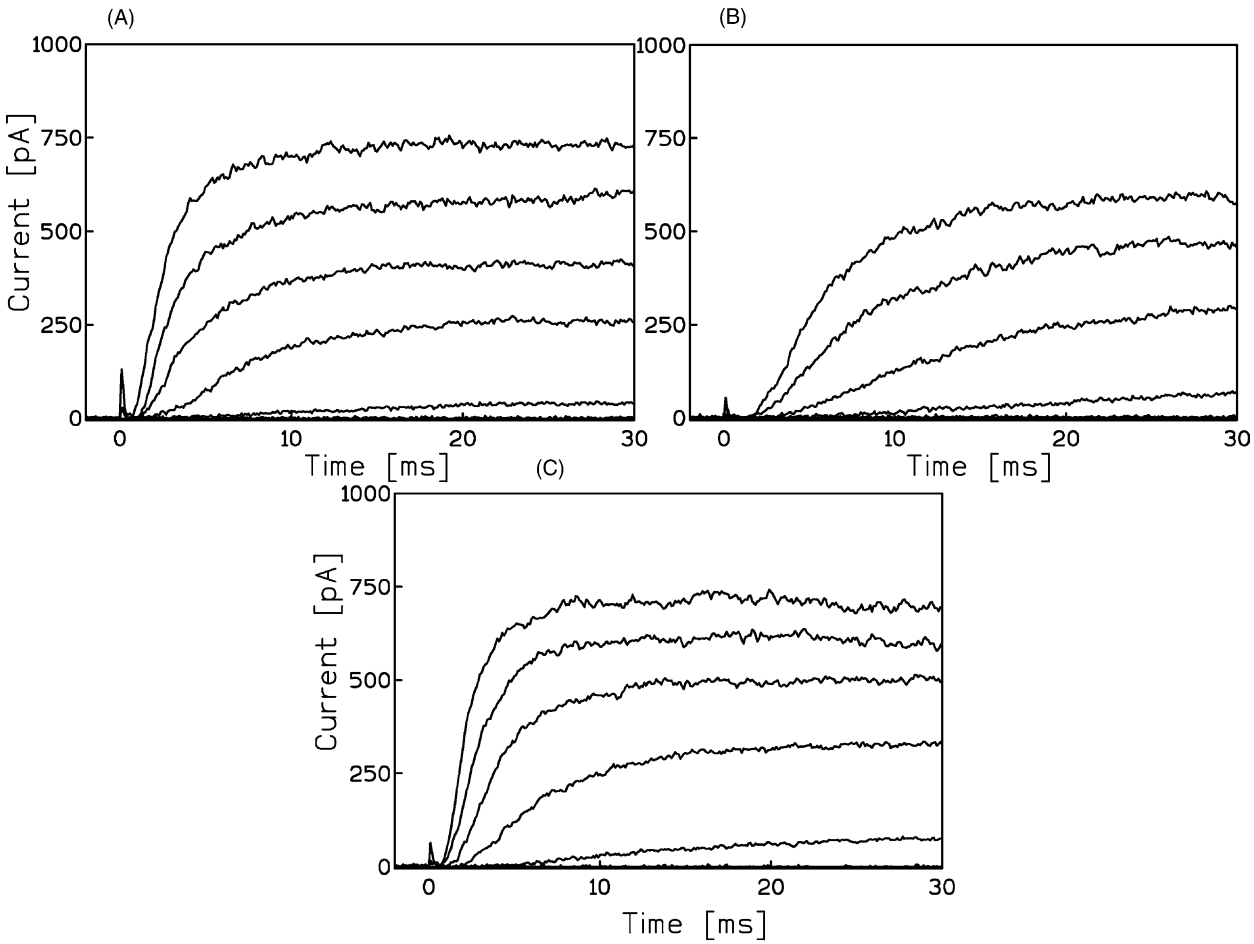

Fig. 2. Whole-cell potassium currents in human TL recorded by applying a standard depolarising voltage protocol described in Section 2. (A) Control conditions, (B) application of 20 μM Zn and (C) wash out.

activation to voltage dependence (k_n) was also affected upon Zn treatment with no clear concentration dependence. The value of k_n was 4.46 ± 3.89 mV (N = 30) under control conditions and was changed to 11.87 ± 1.15 mV (N = 6), 8.44 ± 0.48 mV (N = 6) and 13.75 ± 2.59 mV (N = 30) upon application of 10, 20 and 100 μM Zn, respectively.

Channel deactivation (closure) was also studied by applying the modified tail current protocol described in

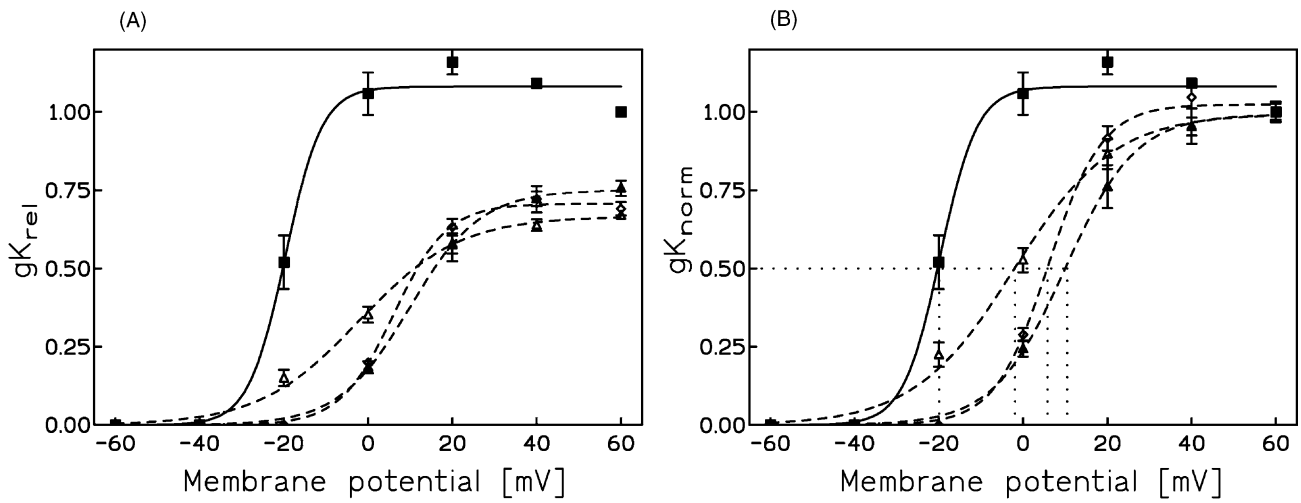

Fig. 3. (A) Steady-state activation plotted as a relative chord conductance vs. the membrane potential. (B) Steady-state activation as a normalised chord conductance vs. the membrane potential. Filled squares: control conditions (N = 30), open triangles: 10 μM Zn (N = 6), filled triangles: 20 μM Zn (N = 6), open diamonds: 100 μM Zn (N = 30).

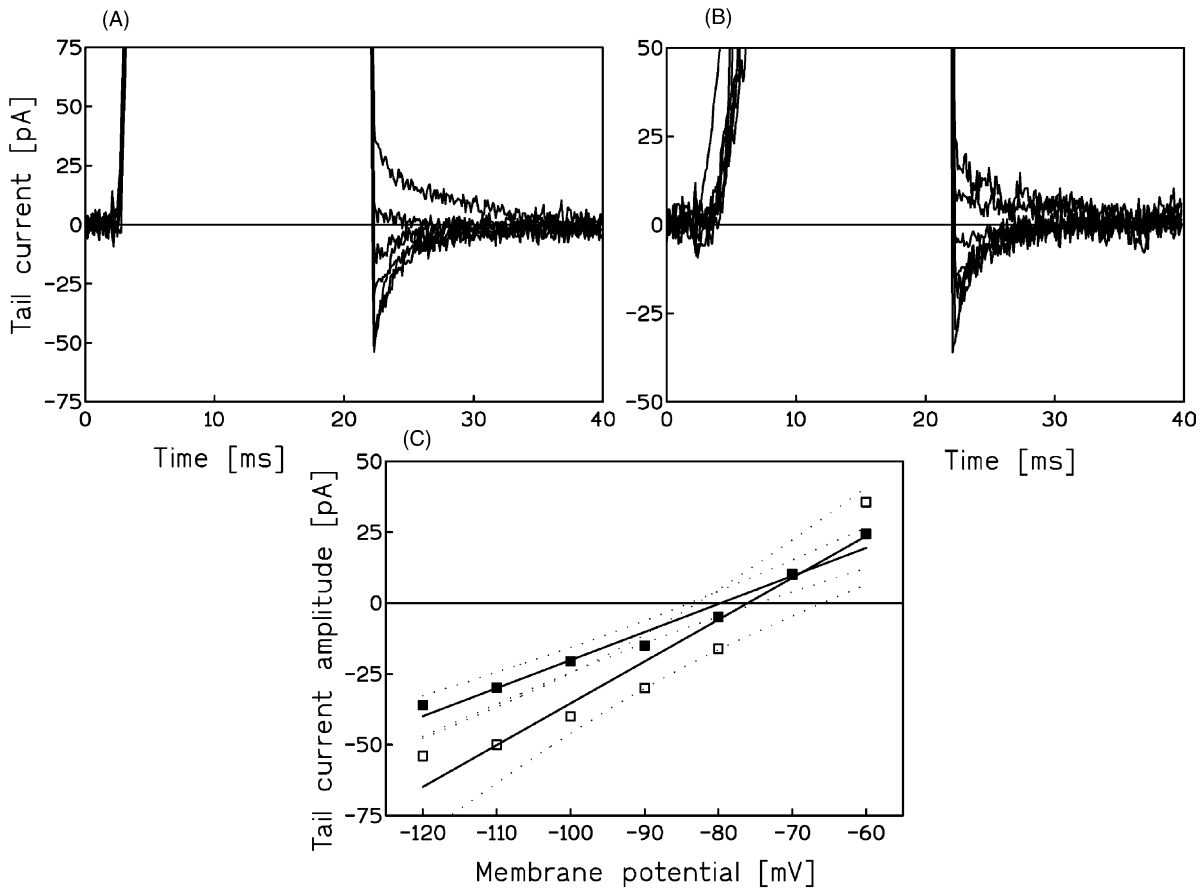

Fig. 4. Tail currents in TL recorded by applying the modified protocol described in Section 2 under: (A) control conditions, (B) application of 100 μM Zn, (C) tail current amplitude plotted as a function of membrane potential. Open squares: control conditions, filled squares: application of 100 μM Zn. The data was fitted by a linear regression.

Section 2. Fig. 4A and B show an example of tail currents recorded under control conditions and upon application of 100 μM Zn, respectively. For clarity, only the first 20 ms of the currents are depicted on the graphs. Fig. 4C shows the tail current amplitude recorded under control conditions and in the presence of 100 μM Zn as the function of membrane potential. A significant reduction of the current amplitude upon Zn treatment due to the channel inhibition can be observed.

Tail currents reversed at the potential of -81.77 ± 3 mV ($N = 5$) under control conditions and at -78.13 ± 4 mV ($N = 5$) upon Zn application. This indicates that, in both cases, the recorded currents are predominantly potassium currents. The rate of tail current decay does not seem to be altered upon Zn application. This was further confirmed by calculating the channel activation and deactivation time constants (see Fig. 5A and B). Both the channel activation and deactivation rates are steeply voltage-dependent. Application of Zn slows markedly the activation rate (see Fig. 5A), whereas the channel deactivation rate remains unaffected upon Zn treatment (see Fig. 5B).

Zinc application also affects the steady-state inactivation (see Fig. 6A). The inactivation midpoint (V_i) is shifted from -53.06 ± 0.44 mV ($N = 10$) under control conditions to -36.05 ± 0.48 mV ($N = 10$) upon application of 100 μM Zn (see Fig. 6A). The steepness of the voltage dependence of the steady-state inactivation curve was changed from -4.24 ± 0.37 mV ($N = 10$) under control conditions to -6.55 ± 0.41 mV ($N = 10$) upon application of 100 μM Zn. Fig. 6B depicts the effect of 100 μM Zn application on the channel inactivation rate. Channel inactivation is much slower than the activation and is weakly voltage-dependent. Contrary to what was observed in case of activation, inactivation rate is not significantly affected upon Zn treatment.

When increasing the zinc concentration to levels higher than 100 μM a significant concentration-dependent reduction of the current amplitude is observed (see Fig. 7A). Application of 100, 300 and 1300 μM Zn reduced the relative chord conductance to 0.74 ± 0.03 ($N = 30$), 0.49 ± 0.032 ($N = 30$) and 0.21 ± 0.014 ($N = 10$) of the control value, respectively. Raising the Zn concentration up to 2.6 mM decreased the conductance to 0.18 ± 0.017 ($N = 6$) of the control value (data not shown). Reversal potential of the currents remained at the level of -80 mV ($N = 6$) even in the presence of 2.6 mM Zn in the external solution (data not shown). This indicates that the currents are not completely blocked upon Zn treatment. The inhibitory effect of Zn on the currents is reversible at all the

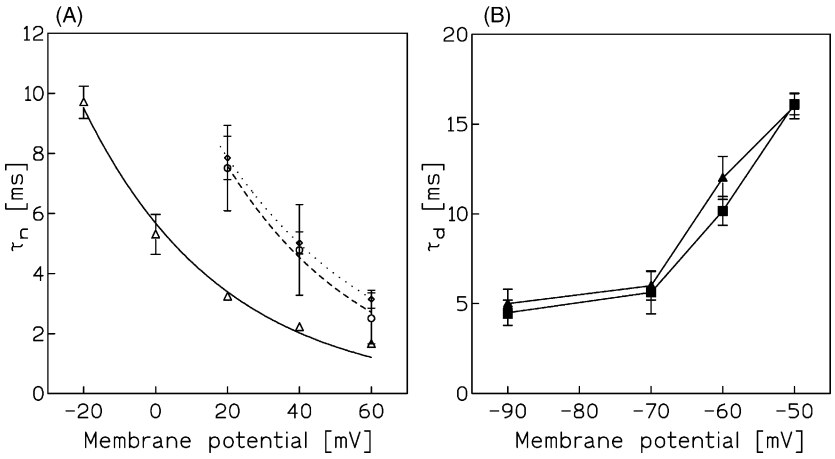

Fig. 5. (A) Activation kinetics of the currents plotted as the activation time constant vs. the membrane potential. The presented data was fitted by an exponential function. Open triangles: control conditions (N = 30), open circles: 100 μM Zn (N = 30), open diamonds: 300 μM Zn (N = 30). (B) Deactivation kinetics plotted as the time constant vs. the membrane potentials. The time constants were calculated by fitting the currents with an exponential function and the data was fitted by a point-to-point line. Filled squares: control conditions (N = 10), filled triangles: application of 300 μM Zn (N = 10).

concentrations tested (data not shown). The observed reduction of the currents is not accompanied by any further change in the channel gating. The activation midpoint value (V_n) is 13.75 ± 2.59 mV (N = 30), 14.10 ± 2.30 mV (N = 30) and 14.28 ± 3.02 mV (N = 10) upon application of 100, 300 and 1300 μM Zn, respectively (see also Fig. 7B). The steepness of the voltage dependence (k_n) is 13.75 ± 2.59 mV (N = 30), 13.81 ± 1.75 mV (N = 30) and 10.66 ± 2.45 mV (N = 10), respectively. Also the activation kinetics remain unchanged when increasing the Zn concentration from 100 to 300 μM (see Fig. 5A) and to higher concentrations (data not shown). Steady-state inactivation, inactivation and deactivation rate are also unchanged in the Zn concentration range from 100 to 2.6 mM (data not shown).

In order to present more clearly the concentration dependence of the current reduction, a semi-logarithmic plot of the fraction of inhibited current as a function of Zn concentration is presented in Fig. 8. The half-blocking concentration of Zn was of 346 ± 40 μM and the Hill coefficient -1.84 ± 0.21.

Since it is known that divalent cations affect the voltage dependence of channel kinetics by modifying the surface potential of cell membrane, additional experiments were performed using external solutions with increased concentrations of Mg and Ca. When rising $CaCl_2$ and $MgCl_2$ to 4 and 5 mM respectively, the Zn effect was indistinguishable from that observed in normal external solution (not shown). This result indicates that Zn exerts its effect by direct interaction with channel macromolecule rather than by affecting the surface potential.

It is known that the gating of Kv1.3 channels is significantly affected by extracellular potassium [21]. Since Zn affects the channel gating and conductance at different

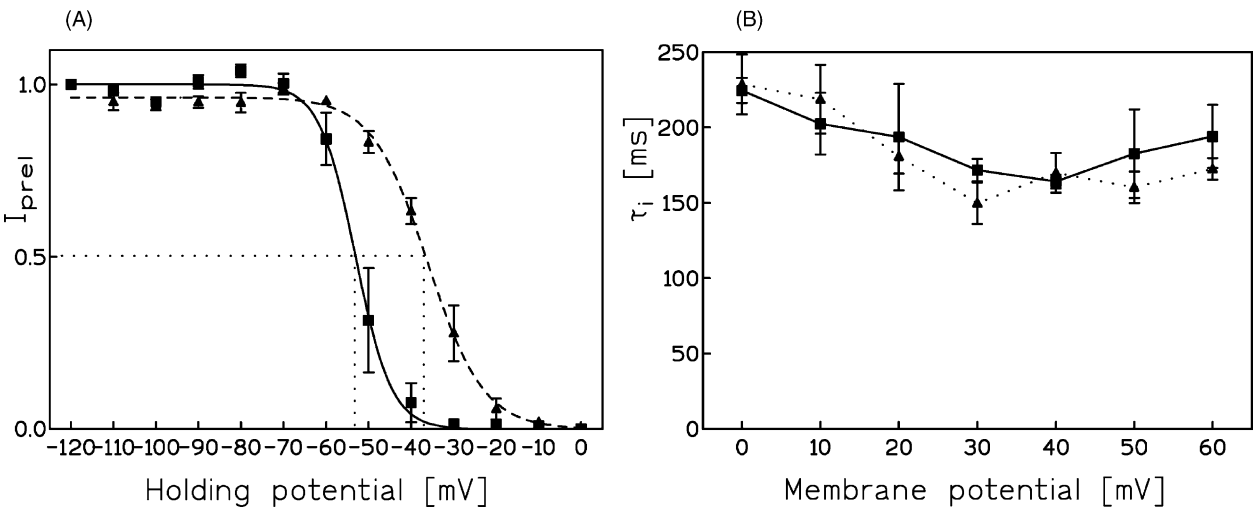

Fig. 6. (A) Steady-state inactivation plotted as the relative peak current recorded at +40 mV vs. the holding potential. (B) Inactivation time constant vs. the membrane potential. The time constants were calculated by fitting the currents with an exponential function and the data was fitted by a point-to-point line. Filled squares: control conditions (N = 10), filled triangles: application of 100 μM Zn (N = 10).

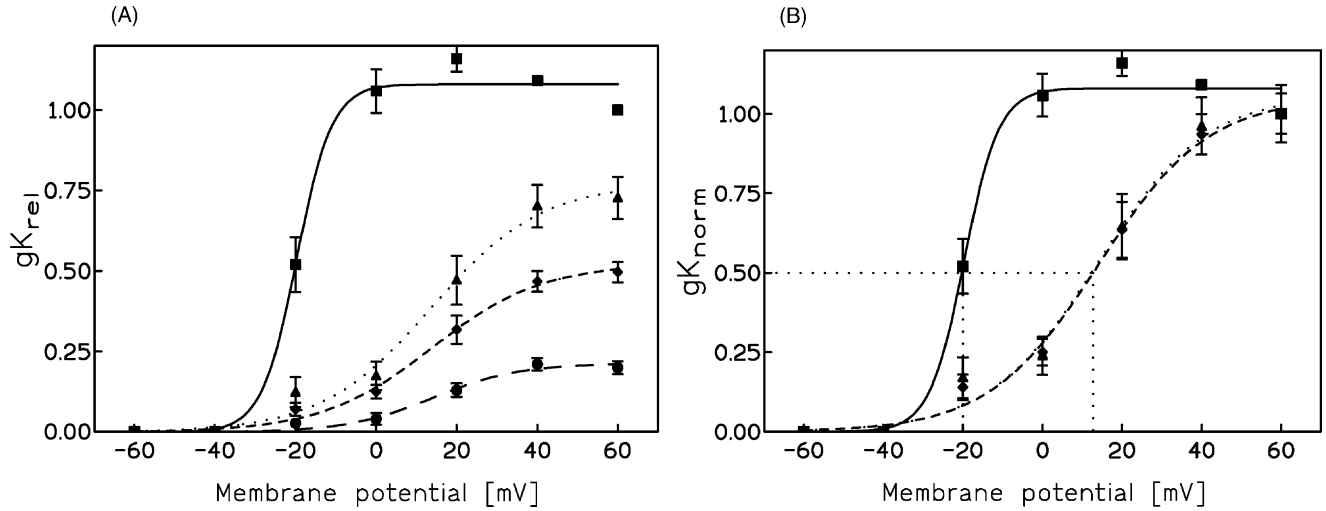

Fig. 7. (A) Steady-state activation plotted as a relative chord conductance vs. the membrane potential. (B) Steady-state activation as a normalised chord conductance vs. the membrane potential. Filled squares: control conditions (N = 30), filled triangles: 100 μM Zn (N = 30), filled diamonds: 300 μM Zn (N = 30), filled circles: 1300 μM Zn (N = 10).

concentrations probably due to action on two different binding sites (see below), it may be expected that an increase in extracellular potassium concentration might differentially modulate Zn-sensitivity of Kv1.3 channel gating and conductance. Therefore, in order to further elucidate the mechanism of zinc influence on Kv1.3 channel activity a series of experiments were additionally carried out in the presence of high potassium concentration (150 mM) in the extracellular solution. Fig. 9A presents an example of whole-cell potassium currents recorded in a TL in the presence of 150 mM K^+ applying the same experimental protocol as defined in Section 2. The currents are inward at the potential of −20 mV, reverse around 0 mV, and are outward at potentials +20 mV and above. These results are in agreement with estimations of the reversal potential obtained by applying the Nernst's equation for extracellular and intracellular potassium concentrations under experimental conditions. The data further confirm

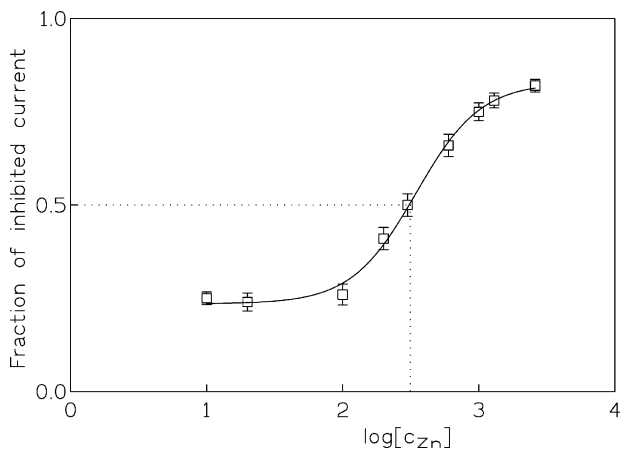

Fig. 8. Semi-logarithmic plot of the degree of current inhibition (a reciprocal of the amplitude of the relative chord conductance) vs. logarithm of zinc concentration.

that the recorded currents are due to an activation of potassium channels and the possibility of a significant contribution of chloride currents to the recorded currents can be ruled out. Fig. 9B depicts the effects of application of 20 μM Zn to the extracellular solution. It can be seen that in the presence of zinc the currents are evoked only at potentials more positive than 0 mV. This suggests that the activation threshold of the channels is shifted towards positive potentials, such as it occurs in the presence of 4.5 mM K^+ (cf Figs. 2B and 9B). Moreover, the activation kinetics of the currents seems to be slower in the presence of zinc. The current amplitude is also reduced in the presence of zinc (cf Fig. 9A and B). However, the amplitude reduction is significantly lower when compared to records obtained under the same Zn concentration in the presence of 4.5 mM K^+ in the extracellular solution (cf Figs 2B and 9B, see below). The effects of Zn are reversible (see Fig. 9C).

Fig. 10A depicts steady-state activation in terms of a normalised chord conductance (defined in Section 2) in the presence of 150 mM K^+ in the extracellular solution. The activation midpoint (V_n) under control conditions is slightly shifted towards negative potentials and is -23.51 ± 5.35 mV (N = 10). This is in agreement with the data obtained by Pahapill and Schlichter [21] that the activation threshold of the channels is shifted towards negative membrane potentials when raising extracellular potassium concentration. The steepness of the steady-state activation to membrane potential curve (k_n) is 3.10 ± 1.59 mV (N = 10). The application of 10, 100 and 300 μM Zn shift the activation midpoint parameter to $+8.98 \pm 3.58$ mV (N = 8), $+15.26 \pm 1.36$ mV (N = 8) and $+10.32 \pm 3.8$ mV (N = 9), respectively. The steepness parameter is changed to 5.06 ± 1.65 mV (N = 8), 9.75 ± 1.89 mV (N = 8) and 8.28 ± 3.09 mV (N = 9), respectively. The activation midpoint parameters obtained

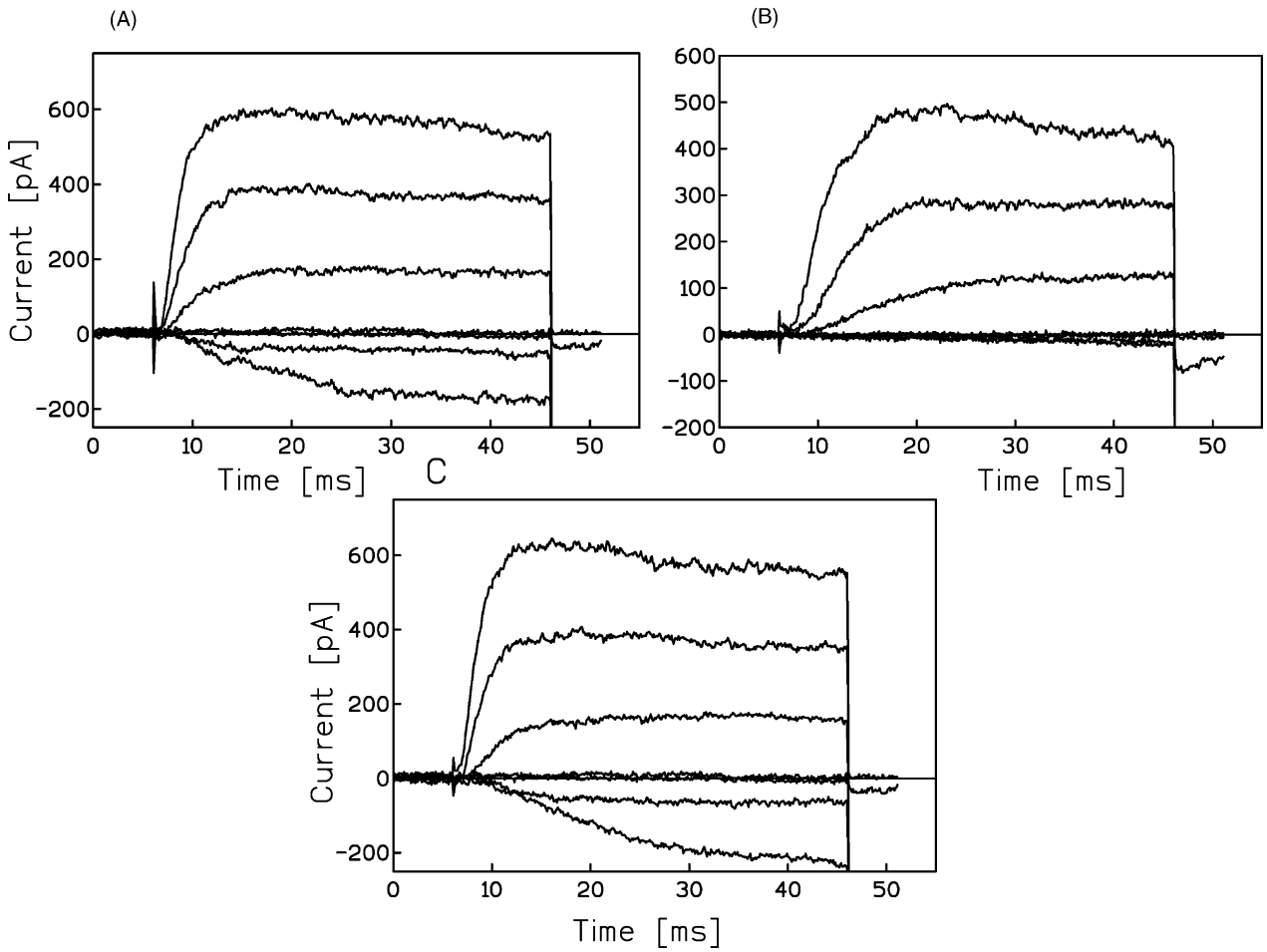

Fig. 9. Whole-cell potassium currents in human TL recorded in the presence of 150 mM K^+ in the extracellular solution by applying a standard depolarising voltage protocol described in Section 2. (A) Control conditions, (B) application of 20 μM Zn, (C) wash out.

for 100 and 300 μM Zn in the presence of 4.5 and 150 mM K^+ in the extracellular solution are not significantly different from each other. This can be better seen on Fig. 10B, which presents the steady-state activation curves obtained for Zn concentrations mentioned above in the presence of 4.5 and 150 mM K^+. When raising zinc concentration to 1 and 2.6 mM in the presence of 150 mM K^+ in the extracellular solution, activation midpoint parameters are

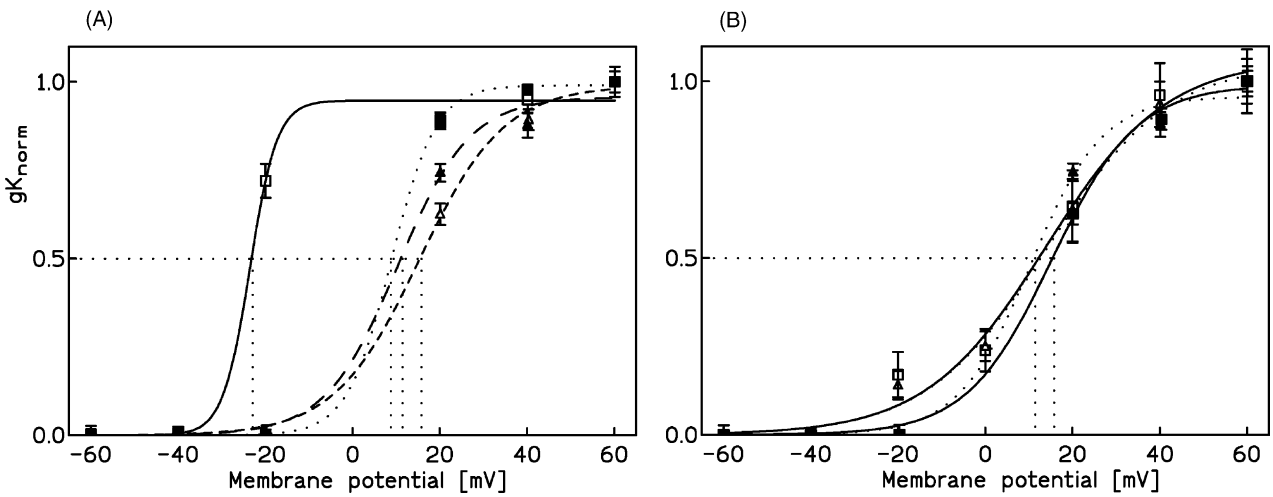

Fig. 10. (A) Steady-state activation as a normalised chord conductance vs. the membrane potential in the presence of 150 mM K^+. Open squares: control conditions (N = 10), filled squares: 10 μM Zn (N = 8), open triangles: 100 μM Zn (N = 8), filled squares: 300 μM Zn (N = 9). (B) Steady-state activation as a normalised chord conductance vs. the membrane potential: open squares: 100 μM Zn (N = 30), 4.5 mM K^+; open triangles: 300 μM Zn (N = 30), 4.5 mM K^+; filled squares: 100 μM Zn (N = 8), 150 mM K^+; filled triangles: 300 μM Zn (N = 9), 150 mM K^+.

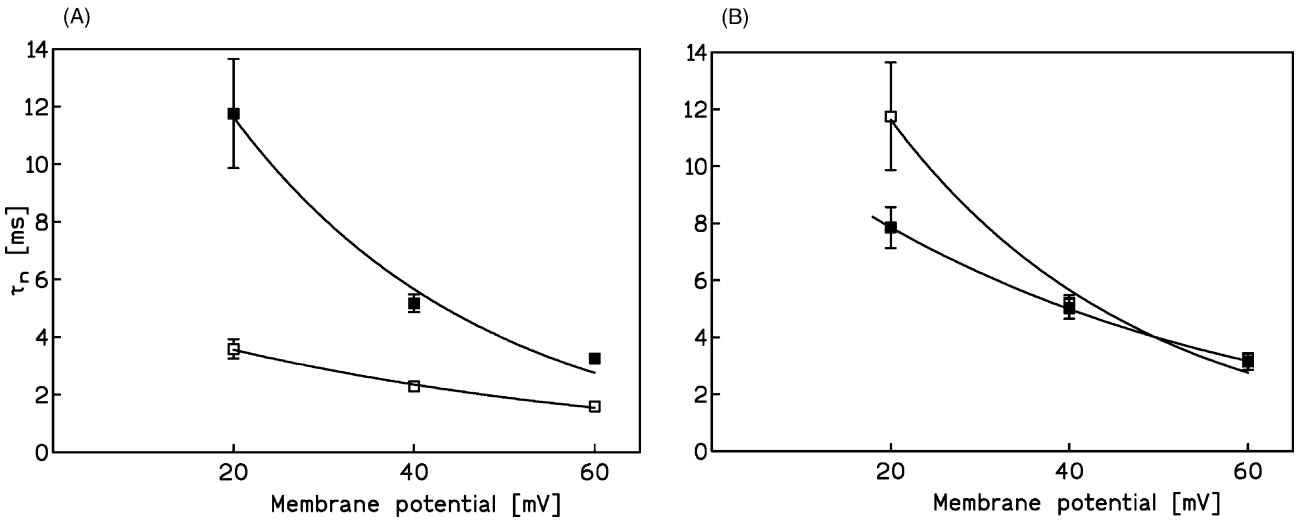

Fig. 11. Activation kinetics as the activation time constant vs. the membrane potential. The presented data was fitted by an exponential function. (A) Open squares: control conditions (N = 10), 150 mM K^+; filled squares: 100 μM Zn (N = 8), 150 mM K^+. (B) Open squares: 100 μM Zn (N = 8), 150 mM K^+; filled squares: 100 μM Zn (N = 30), 4.5 mM K^+.

$+18.67 \pm 0.53$ mV (N = 10) and $+13.13 \pm 2.94$ mV (N = 6), respectively, and steepness parameters are 8.95 ± 0.93 mV (N = 10) and 10.20 ± 3.22 mV (N = 6), respectively. Also in this case the activation midpoint parameters do not differ significantly from those obtained for comparable zinc concentrations in the presence of 4.5 mM K^+ in the extracellular solution.

It is known that zinc application also slows the kinetics of current activation. Fig. 11A depicts activation time constants as a function of membrane potential in the presence of 150 mM K^+ under control conditions and upon application of 100 μM Zn. Raising the zinc concentration up to 2.6 mM does not influence the activation kinetics more significantly than at 100 μM (data not shown). Fig. 11B shows the activation kinetics upon 100 μM Zn application in the presence of 4.5 and 150 mM K^+ in the extracellular solution. Activation time constants are significantly different from each other only at the potential of +20 mV and this may be due to a scatter of the data obtained in the presence of 150 mM K^+. At the potentials of +40 and +60 mV the data obtained in the presence of 4.5 and 150 mM K^+ are almost identical (see Fig. 11B).

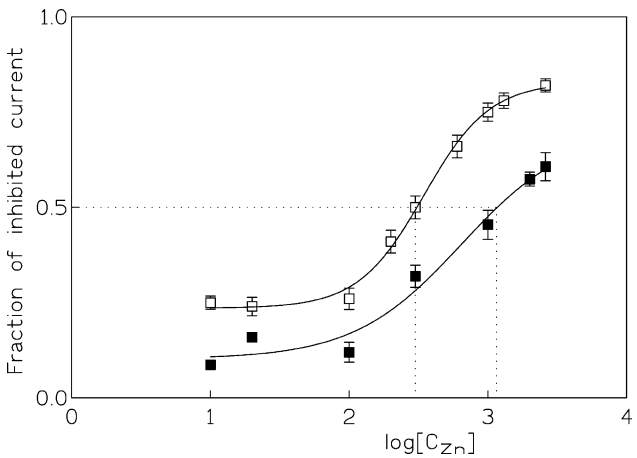

Fig. 12. Semi-logarithmic plot of the fraction of the inhibited current vs. logarithm of zinc concentration: open squares: 4.5 mM K^+; filled squares: 150 mM K^+.

Peak currents are also reduced upon zinc application in the presence of 150 mM K^+ in the extracellular solution. However, in contrast to the steady-state activation and activation kinetics, the degree of current inhibition is significantly diminished. Application of 10, 20, 100, 300 μM; 1, 2 and 2.6 mM Zn in the presence of 150 mM K^+ reduces the peak current at the potential of +60 mV to 0.91 ± 0.014, 0.84 ± 0.0095, 0.88 ± 0.026, 0.68 ± 0.029, 0.54 ± 0.0078, 0.43 ± 0.018 and 0.39 ± 0.037 of the control value, respectively. Fig. 12 depicts a fraction of inhibited currents plotted as a function of a logarithm of zinc concentration in the presence of 150 and 4.5 mM K^+ in the extracellular solution. In the presence of 150 mM K^+ the channels are half-blocked only at a zinc concentration of ca. 1 mM (an adequate estimation is not possible because of a large standard error) and the Hill coefficient is reduced to ca. 1.18 (more adequate estimation not possible). Moreover, our data demonstrate that raising the zinc concentration to 2.6 mM inhibits only ca. 60% of the currents in the presence of 150 mM K^+, whereas ca. 80% of the currents are inhibited in the presence of 4.5 mM K^+. Altogether, the obtained data indicate that the inhibitory effect of Zn is significantly diminished in the presence of 150 mM K^+ in the extracellular solution.

4. Discussion

In the present study, we demonstrate that application of zinc at micromolar concentration reduces TL Kv1.3 channel currents. The reduction of the current amplitude is

accompanied by a shift of both steady-state activation and inactivation towards more positive membrane potentials and a considerable slowing of channel activation kinetics, whereas the channel inactivation and deactivation rate remained unaffected upon Zn treatment. The blocking effect is not complete and the reversal potential of the currents remained unchanged at the level of −80 mV even upon application of 2.6 mM Zn. This indicates that Zn reduces the channel activity but does not completely block the channels at micromolar concentrations. The inhibitory effect of zinc on the currents is significantly diminished when raising extracellular potassium concentration to 150 mM, whereas the shift of the activation threshold and slowing of the activation kinetics remain unchanged.

When recording the whole-cell currents in TL, chloride currents due to an activation of ''maxi'' voltage-gated chloride channels appear additionally to the potassium currents [20]. However, the reversal potential for chloride ions was estimated to be ca. −35 mV under our experimental conditions. That value is far from −80 mV estimated for the recorded currents. That argue against any significant contribution of the chloride current to the total whole-cell current. Moreover, Zn was shown to completely block the whole-cell chloride current in TL at a concentration of 200 μM [20]. Therefore, the hypothesis that the chloride currents may contribute to residual currents upon application of Zn at concentrations higher than 200 μM can be ruled out.

It has long been known that divalent cations alter the gating kinetics in ion channels. This effect was originally described in terms of the surface charge theory first proposed by Frankenhäuser and Hodgkin in 1957 [22]. Our results, however, argued against the concept of zinc action on fixed surface charges. First, our data demonstrate that Zn application shifted markedly steady-state activation curve towards more positive potentials and slowed the channel activation rate without significantly affecting the deactivation process. In contrast, according to the surface charge theory, comparable changes in both activation and deactivation kinetics would be expected. Moreover, in order to eliminate the possibility that Zn might act on fixed surface charges, some of our experiments were performed using a modified external solution with increased concentrations of divalent cations and results obtained using both solutions were indistinguishable from each other. This may suggest specific interactions of zinc ions with channel gating mechanism rather than non-specific interactions of divalent cations on fixed surface charges.

It is known that divalent and trivalent heavy metal cations interact with Kv1.3 channels, inhibit the currents and alter the channel gating [10–14]. These effects were first studied by DeCoursey *et al.*, who showed that the cations inhibited the whole-cell currents with a relative potency from most potent to least potent: Hg > La > Zn, Co > Ba, Cd > Mn, Ca > Sr > Mg [10]. The inhibitory effect of Ni had been reported earlier by Matteson and Deutsch [23]. The cations acted at different concentrations varying from 1 μM for Hg and La to 100 mM for Sr and Mg [10]. Application of the cations also produced a shift of the channel activation threshold towards more positive potentials, that effect was most pronounced upon La treatment [10]. Moreover, the studies demonstrated that the cations differently affected the channel inactivation rate: inactivation was accelerated upon application of La, Ca, Sr, Ba and slowed in the presence of Ni, Co, Cd and Mn [10–14]. Our results demonstrate that the channel inactivation rate is not significantly affected upon Zn treatment. This may indicate that the mechanism of Zn interaction with the channel is different from heavy metals listed above.

Results of our study demonstrate that raising the zinc concentration to levels higher than 100 μM produces an additional concentration-dependent inhibitory effect on the current amplitude with a half-blocking concentration of 346 μM and this effect occurs without any change in the channel gating. This may indicate that zinc affects the channel gating and current independently due to actions on two different binding sites. Binding to one site that is saturated at concentrations higher than 20 μM affects the channel gating: shifts both steady-state activation and inactivation towards more positive membrane potentials and slows the channel activation kinetics considerably. Binding to another site at concentrations higher than 100 μM inhibits the currents without affecting the channel gating.

The results obtained in the presence of 150 mM K^+ in the extracellular solution may support the hypothesis that zinc acts on two different binding sites. Results of our study demonstrate that the effects of zinc treatment on both the steady-state activation and activation kinetics remain unchanged when raising extracellular potassium concentration. In contrast, obtained data demonstrate that the inhibitory effect of zinc on the currents is significantly diminished in the presence of 150 mM K^+ in the extracellular solution. Altogether, our data may suggest that the changes in channel gating and the reduction in peak current are due to zinc interactions with two different binding sites. Binding to the site that alters the gating parameters is not affected by extracellular potassium, whereas binding to the site that blocks the current is significantly inhibited by potassium ions.

Zn affects many types of voltage-gated potassium channels including related Kv1.1, Kv1.4 and Kv1.5 channels stably expressed in transfected mouse fibroblasts [8]. Application of Zn at micromolar concentrations shifted the steady-state activation curves for all the three channels towards more positive potentials and this was accompanied by a considerable reduction of the whole-cell potassium current [8]. Moreover, Zn application shifted the steady-state inactivation curve for Kv1.4 channels towards more positive potentials and slowed considerably the activation kinetics of Kv1.5 channels [8]. Results recently obtained

for Kv1.5 channels suggest the existence of two independent binding sites for zinc—binding to one site affects the channel gating and binding to another site inhibits the current [24,25]. In case of Kv1.1 channels it was proposed that a single binding site might be responsible for the changes in channel gating upon Zn treatment [8]. Results of our study demonstrate that application of Zn at micromolar concentrations reduces the Kv1.3 channel activity and affects the channel gating. Moreover, our results suggest that two different sites may be involved in Zn binding. It can be concluded that, although the effects of Zn on Kv1.1, Kv1.3, Kv1.4 and Kv1.5 macroscopic currents are similar, the mechanism of Zn interactions with the channels is different and binding to one or two different sites might be involved in the observed changes in channel gating and current.

The modulatory effects on Kv1.3 channels may be related to influence of Zn on TL function. The total concentration of Zn in the horse plasma was estimated to be about 8 μM, however Zn ions are mostly bound to albumin, so the plasma concentration of free Zn is in submicromolar range [26]. Such a small concentration of Zn may be too low to exert any effects on Kv1.3 channels. Nevertheless, Zn plays an important role in the function of the immune system—Zn deficiency is related to thymic atrophy, lymphopenia and alterations in the proportions of the various subsets of lymphocytes and mononuclear phagocytes [27]. As a result, antibody-mediated responses to both T cell-dependent and -independent antigens are significantly reduced [27]. Cytolytic T cell responses, natural killer cell activity and delayed-type hypersensitivity reactions are also depressed [27]. Whether or not these effects of Zn deficiency are related to interactions of Zn with Kv1.3 channels remains to be investigated. The modulatory effects on Kv1.3 channels may underlie mitogenic effects of Zn occurring *in vitro* [28]. It is known that Zn stimulates T cell mitogenesis both in human and murine TL [28,29]. The mitogenic effect of Zn is dose- and time-dependent, giving an optimal effect at 200 μM Zn concentration and for the incubation period of 144 hr [28]. Interestingly, Zn inhibits the TL mitogenesis when applied at higher concentrations (800 μM). [28]. The exact mechanisms of these effects remain unknown. Results of our study demonstrate that application of 200 μM Zn shifts the channel activation threshold towards more positive potentials. Moreover, it is known that the resting membrane potential in quiescent TL is set primarily by the activity of Kv1.3 channels [9]. It is therefore likely that Zn application at concentrations mentioned above may result in a depolarisation of TL cell membrane. It was shown that the TL cell membrane is depolarised from the resting level of ca. −65 mV to ca. −25 mV during the first 2–4 hr following mitogenic stimulation [30]. This was suggested to be one of the initial key events during T cell activation [31]. It is therefore possible that the stimulatory effect of Zn on TL cell mitogenesis may be related to the depolarisation of TL cell membrane due to the shift of the Kv1.3 channel activation threshold towards more positive potentials. On the other hand, it is known that the TL cell mitogenesis is inhibited by Kv1.3 channel blockers [9]. Results of our study demonstrate that application of Zn at concentrations higher than 100 μM produces a concentration-dependent inhibition of the currents additionally to the changes in channel gating. The inhibitory effects on the cell mitogenesis exerted by Zn at concentration of 800 μM may thus be related to the blocking effect on Kv1.3 channels.

Modulation of Kv1.3 channels activity may also contribute to the modulatory effects of zinc on neuronal activity. Kv1.3 channels are also present in rat and mouse brain cells [9]. It is known that Zn is present in many regions of the central nervous system and some regions, such as mossy fibre terminals of the hippocampus are especially rich in Zn [32]. Zn concentration at synapses in the CA3 subfield of the hippocampus was estimated to be within the range of 100–300 μM, whereas in other regions of the brain Zn is present at much lower levels (1–20 μM) [32]. Results of our study demonstrate that application of 10–20 μM Zn is sufficient to alter the Kv1.3 channel gating and raising the Zn concentration up to 300 μM not only affect the channel gating, but also reduces the current amplitude to less than 50% of the control value. Therefore, both the alterations in the channel gating and the reduction of the currents are likely to appear under physiological conditions and may contribute to modulatory effects on neuronal activity in the presence of Zn.

Acknowledgments

The authors would like to express best thanks to our colleague from the Biophysics Department—Dr. Andrzej Poła, who kindly provided the blood samples for lymphocyte isolation. This work was supported by the Wrocław Medical University Grant (Grant Uczelniany) No. 561.

References

[1] Harrison NL, Gibbons SJ. Zinc: an endogenous modulator of ligand and voltage-gated ion channels. Neuropharmacology 1994;33:935–52.
[2] Gilly F, Armstrong CM. Divalent cations and the activation kinetics of potassium channels in squid giant axons. J Gen Physiol 1982;79:965–96.
[3] Spires S, Begenisich T. Chemical properties of the cation binding site on potassium channels. J Gen Physiol 1992;100:181–93.
[4] Spires S, Begenisich T. Modulation of potassium channel gating by external divalent cations. J Gen Physiol 1994;104:675–92.
[5] Huang R, Peng Y, Yau K. Zinc modulation of a transient potassium current and histochemical localization of the metal in neurons of the suprachiasmatic nucleus. Proc Natl Acad Sci USA 1993;90:11806–10.
[6] Bardoni R, Belluzzi O. Modifications of A-current kinetics in mammalian central neurones induced by extracellular zinc. J Physiol 1994;479:389–400.

[7] Erdelyi L. Zinc modulated A-type potassium currents and neuronal excitability in snail neurons. Cell Mol Neurobiol 1994;14:689–99.
[8] Harrison NL, Radke HK, Tamkun MM, Lovinger DM. Modulation of gating of cloned rat and human K^+ channels by micromolar zinc. Mol Pharmacol 1992;43:482–6.
[9] Lewis RS, Cahalan MD. Potassium and calcium channels in lymphocytes. Annu Rev Immunol 1995;13:623–53.
[10] DeCoursey TE, Chandy KG, Gupta S, Cahalan MD. Voltage-dependent ion channels in T lymphocytes. J Neuroimmunol 1985;10:71–95.
[11] DeCoursey TE, Chandy KG, Gupta S, Cahalan MD. Two types of potassium channels in murine T lymphocytes. J Gen Physiol 1987;89:379–404.
[12] Grissmer S, Cahalan MD. Divalent ion trapping inside potassium channels in human T lymphocytes. J Gen Physiol 1989;93:609–30.
[13] Douglass J, Osborne P, Cai-cai Y, Wilkinson M, Christie M, Adelamn JP. Characterization and functional expression of a rat genomic DNA clone encoding a lymphocyte potassium channel. J Immunol 1990; 144:4841–50.
[14] Cai-cai Y, Osborne P, North R, Dooley D, Douglass J. Characterization and functional expression of genomic DNA encoding the human lymphocyte type n potassium channel. DNA Cell Biol 1992;11: 163–72.
[15] Teisseyre A, Mozrzymas JW. Extracellular zinc inhibits the activity of Kv1.3 channels in human T lymphocytes. In: Proceedings of the Symposium on Biophysics and Biology of Environmentally Important Membrane-Active Compounds, 2001 May 11–13; Wrocław, Poland. Cell Mol Biol Lett 2001;6:425.
[16] Hirano T, Kuritani T, Kishimoto Y, Yamamura Y. T cell dependency of PWM-induced Ig production by B cells. J Immunol 1977;119: 1235.
[17] Hamill O, Marty A, Neher E, Sakmann B, Sigworth F. Improved patch-clamp techniques for high-resolution current recording from cells and cell-free membrane patches. Pflügers Arch 1981;391:85–100.
[18] Zegarra-Moran O, Basola A, Rogolo M, Porcelli A, Rossi B, Galietta L. HIV-1 Nef expression inhibits the activity of a Ca-2+ dependent K^+ channel involved in the control of the resting potential in CEM lymphocytes. J Immunol 1999;162:5359–66.
[19] Ghanshani S, Wulff H, Miller M, Rohm H, Neben A, Gutman G, Cahalan MD, Chandy KG. Up-regulation of the IKCa1 potassium channel during T-cell activation. J Biol Chem 2000;275:327137–49.
[20] Pahapill PA, Schlichter LC. Cl^- channels in intact human T lymphocytes. J Membr Biol 1992;125:171–83.
[21] Pahapill PA, Schlichter LC. Modulation of potassium channels in intact human T Lymphocytes. J Physiol Lond 1992;445:407–30.
[22] Frankenhäuser B, Hodgkin A. The action of calcium on the electrical properties of squid axons. J Physiol 1957;137:218–44.
[23] Matteson D, Deutsch C. K channels in T lymphocytes—a patch-clamp study using monoclonal antibody adhesion. Nature 1984;307:468–71.
[24] Zhang S, Kwan C, Fedida D, Kehl S. External K^+ relieves the block but not the gating shift caused by Zn in human Kv1.5 channels. J Physiol 2001;532:349–58.
[25] Zhang S, Kehl S, Fedida D. Modulation of Kv1.5 potassium channel gating by extracellular zinc. Biophys J 2001;81:125–36.
[26] Magneson G, Puvathingal JM, Ray WJ. The concentrations of free Mg and free Zn in equine blood plasma. J Biol Chem 1987;262:11140–8.
[27] Fraker PJ, Gershwin ME, Good RA, Prasad A. Interrelationships between zinc and immune function. Fed Proc 1986;45:1474–9.
[28] Reardon CL, Lucas DO. Heavy-metal mitogenesis: Zn and Hg induce cellular cytotoxicity and interferon production in murine T lymphocytes. Immunobiology 1987;175:455–69.
[29] Rühl H, Kirchner H. Monocyte-dependent stimulation of human T cells by zinc. Clin Exp Immunol 1978;32:484.
[30] Kiefer H, Blume AJ, Kaback HR. Membrane potential changes during mitogenic stimulation in mouse spleen lymphocytes. Proc Natl Acad Sci USA 1980;77:2200–4.
[31] Maltsev VA. Oscillating and triggering properties of T cell membrane potential. Immunol Lett 1990;26:277–82.
[32] Frederickson CJ, Klitenick MA, Menton WI, Kirpatrick JB. Cytoarchitectonic distribution of zinc in the hippocampus of man and the rat. Brain Res 1983;273:335–9.